Decision Fusion for Reliable Flood Mapping using Remote Sensing Images

Chandrama Dey, Xiuping Jia and Donald Fraser
School of Information Technology and Electrical Engineering
University College, Australian Defence Force Academy
The University of New South Wales
Canberra, ACT 2600 Australia
Chandrama.Dey@student.adfa.edu.au

Abstract

Flood extent mapping is a basic tool for flood damage assessment, which can be done by digital classification techniques using satellite imageries, including the data recorded by radar and optical sensors. However, converting the data into the information we need is not a straightforward task. One of the great challenges involved in the data interpretation is to separate the permanent water bodies and flooding regions, including both the fully inundated areas and the wet areas where trees and houses are partly covered with water. This paper adopts the decision fusion technique to combine the mapping results from radar data and the NDVI data derived from optical data. An improved capacity in terms of identifying the permanent or semi-permanent water bodies from flood inundated areas has been achieved. Computer software tools Multispec and Matlab were used.

Key Words: remote sensing, classification, decision fusion, flood extent mapping.

1. Introduction

Since time immemorial, rivers have provided great attraction to scholars as well as providing the precious resource of all living beings, water. But this shows only one side of the coin. A river can be furious at times; it can also create floods, a devastating phenomenon of the earth. To understand floods well, first the hazards need to be highlighted. Flooding is the most common and frequent of all natural hazards in Australia [1]. It can be regarded as the most deadly and disastrous in terms of human and economic losses.

It is critical to be able to capture the maximum flood extent during and after any flood event via flood extent mapping. The quantitative mapping results are valuable for flood damage assessment, flood model development and risk analysis.

In recent years, remote sensing technology has made substantial contribution in every aspect of flood disaster management, such as preparedness, prevention and relief. Satellites like IRS-1C/1D with three sensors PAN, LISS-3, and WiFS; NOAA (AVHRR) and Landsat ETM+ provide data for various flood characteristics. Generally speaking, Synthetic Aperture Radar (SAR) images (an active microwave sensor) allow day and night data collection and are independent of weather conditions and illumination. However, they can be difficult to use for differentiating land and water bodies due to the effect of variables on backscattering characteristics. Optical images are relatively easy to interpret. The main concern is that they are often covered by clouds. Other types of spatial data have been adopted for flood inundation mapping as well. As for example, DEM data (digital representations of ground surface topography in a raster form) and river gauge data were used in order to map the 1999 flood extent in the Greenville area [2].

There are a number of automatic information extraction algorithms that have been developed over the years in order to extract the hidden information from imagery [3]. Some are pixel based multispectral classification algorithms. Among them Maximum Likelihood classifier, characterized as a parametric classifier, is widely used. For flood extents mapping several other techniques have been applied to SAR images. For example, level slicing is a traditional method of delineating flooding in non-forested areas. Active contour models or snakes have recently gained popularity as a means of turning incomplete and noisy edge maps into smooth continuous vector segment boundaries [4] .This technique was applied to delineate

the flood boundary from SAR imagery of the two reaches of the river Thames [5].

One of the great challenges involved in the data interpretation is to separate the permanent water bodies and flooding regions, including both the fully inundated areas and the 'wet areas' where trees and houses are partly covered with water. This paper adopts the decision fusion technique to combine the mapping results from radar data and optical data. Theory of Evidence [6] is applied in the decision fusion where the uncertainties of the two data sources are taken into account. An improved capacity in terms of identifying the permanent or semi-permanent water bodies from flood inundated areas has been achieved.

2. Methodology

Figure 1 shows the flow chart of the data processing. Both radar data and optical data are analyzed separately and then the individual decisions made are fused to form a final flood mapping.

Supervised classification techniques such as Maximum likelihood classification, can be applied to the radar data. The maximum likelihood technique assumes each class data follows a normal distribution and works reliably, as long as there are enough training samples [6]. Considering a large flooding extent, the training fields can often be easily obtained and the assumption of normal distribution is generally acceptable.

As illustrated below, it is difficult to separate flooded areas from the permanent water body using radar data alone. Optical data should be used as well, from which NDVI (Normalized Difference Vegetation Index) can be derived using the measurements at the near infrared band (NIR) and the red band (RED). The formula for generating NDVI is as follows.

$$NDVI = (NIR-RED) / (NIR+RED) \quad (1)$$

Non-vegetated areas like water bodies have low NDVI values and consequently can be identified effectively in this way.

Several conventional classification techniques have been tested on radar images for the extraction of the extent of flooding. Level Slicing technique has been applied on optical Landsat images to extract the permanent water body from the study area in order to use this ancillary result on flood images for the accurate mapping of the flooding.

Using Multispec software tools, both supervised and unsupervised classification were attempted to classify the image into flooded and non-flooded regions.

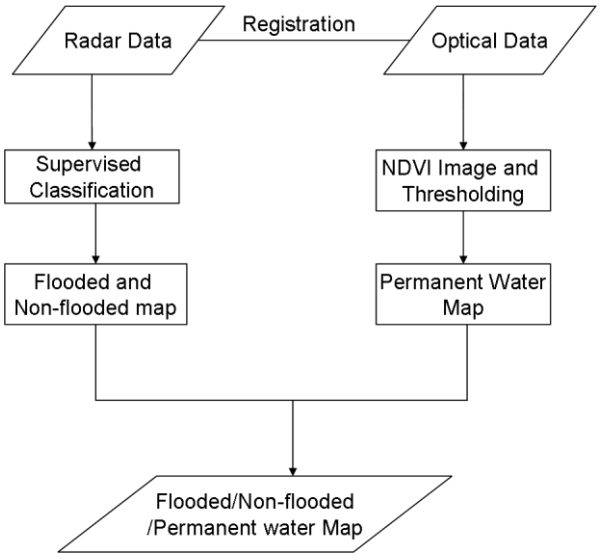

Figure 1. Methodology – radar and optical data processing followed by decision fusion

3. Study area and data

The study area covers the Kendrapara district and extends towards the south, in Orissa state, India. It lies in the river delta formed by the Brahmani and Baitarani rivers. The location of the study area is approximately from $20^0$18' N to $20^0$28'30'' N and $86^0$2' E to $86^0$37' E respectively.

Remotely sensed data used in this study are Landsat ETM (30 metres) of 23rd October, 2000 and Radarsat (50 metres) of 4th September, 2003. Although Landsat ETM images have 8 bands, for the purpose of extracting the permanent water body only the near infrared, red and green bands were used. This image is the pre-flood image whereas the Radarsat image was taken during the flood.

During the fieldwork, ground truths and evidences regarding the actual flooded area and other natural depressions were collected. One interesting characteristics of the study area was observed in that there are several water bodies that are covered with aquatic plantation and dense canopy (Figure 2). It was also observed that open areas (roads) are un-metalled except for some major highways beyond the study area.

Figure 2. The canopy covered water body

4. Data analysis

4.1. Supervised classification

Initially the Maximum likelihood classification was run on the radar image to map Flooded (including permanent water bodies) and Non-flooded regions. Eight training fields were chosen (four for each class) and their accuracies were assessed to test the class model. The testing fields were also selected and classified to test if the class models are good for data other than training data. The accuracy obtained will allow a degree of confidence to be attached to the results and will serve to indicate whether the analysis objectives have been achieved. Accuracy is determined empirically, by selecting a sample of pixels from the thematic map and checking their labels against classes determined from reference data (from field observation). From these checks the percentage of pixels from each class in the image labeled correctly by the classifier can be estimated along with the proportions of pixels from each class erroneously labeled into every other class. These results are represented in a tabular form, often referred to as Confusion or Error matrix [6]. The accuracy for the training data and testing data are given in Table 1 and Table 2, respectively.

Table 1. Classification performance on training data (re-substitution method)

Project Class Name	Class number	Reference Accuracy(%) (producer's accuracy)	Number of Samples	Number of Samples in thematic Image class	
Flooded	1	98.0	1229	1204	25
Non-flooded	2	99.8	3163	6	3157
Total			4392	1210	3182
Reliable Accuracy(%) (user's accuracy)				99.5	99.2
OVERALL CLASS PERFORMANCE (4361/4392)=99.3% Kappa Statistic(x100)=98.2% Kappa Variance=0.000010					

Table 2. Class performance on testing data

Project Class Name	Class number	Reference Accuracy(%) (producer's accuracy)	Number of Samples	Number of Samples in thematic Image class	
Flooded	1	100	428	428	0
Non-flooded	2	100	2036	0	2036
Total			2464	428	2036
Reliable Accuracy(%) (user's accuracy)				100	100
OVERALL CLASS PERFORMANCE (2464/2464)=100.0% Kappa Statistic(x100)=100% Kappa Variance=0.000000					

As observed, the accuracy of the training data was 99.3% and the kappa Statistic of 98.2%. For the testing data, both accuracy level and the Kappa Statistic are 100%.

The histogram of the training data also shows two distinctive classes of flooded and non-flooded areas (Figure 3). After testing, the whole image was classified using the estimated parameters. Figure 4 shows the classification map obtained.

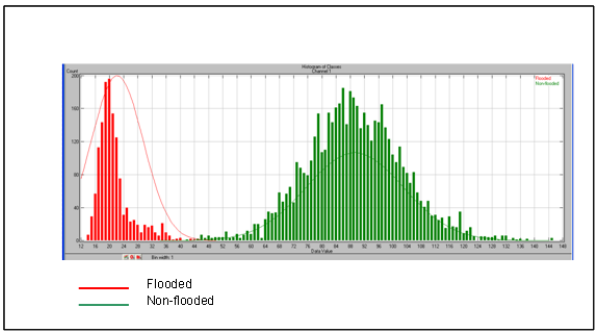

Figure 3. The histogram showing the class distinctiveness

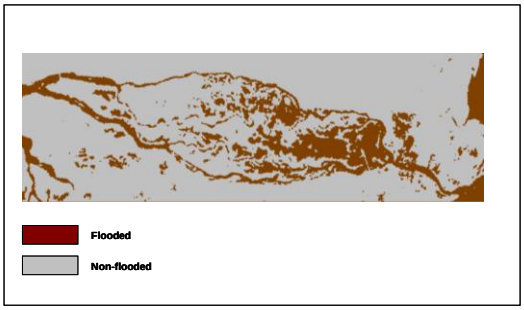

Figure 4. The classification into flooded and non-flooded areas

A second experiment has been conducted which classifies the image into 3 classes of Flooded, Non-flooded and Permanent water body. Through this classification an attempt has made to extract the permanent water bodies from the flooded portions. The Error Matrix of the training classes falls down to 88.7% with Kappa Statistic of only 77.8% (Table 3).
The Error Matrix for the test classes shows that although the overall accuracy is about 94.2%, it is only for the accurate classification of the Non-flooded area and flooded area. The extraction of permanent water body is not satisfactory. The Kappa Statistic is 84.3% (Table 4).

Table 3. Training class performance (re-substitution method)

Project Class Name	Class number	Reference Accuracy(%) (producer's accuracy)	Number of Samples	Number of Samples in thematic Image class		
Flooded	1	67.5	1229	829	375	25
Permanent water body	2	69.4	470	138	326	6
Non-flooded	3	99.8	3163	6	0	3157
Total			4862	973	701	3188
Reliable Accuracy(%) (user's accuracy)				85.2	46.5	99.0
OVERALL CLASS PERFORMANCE (4312/4852)=88.7% Kappa Statistic(x100)=77.8% Kappa Variance=0.000063						

Table 4. Test classification performance

Project Class Name	Class number	Reference Accuracy(%) (producer's accuracy)	Number of Samples	Number of Samples in thematic Image class		
Flooded	1	83.7	356	298	33	25
Permanent water body	2	57.2	180	73	103	4
Non-flooded	3	100.0	1778	0	0	1778
Total			2314	371	136	1807
Reliable Accuracy(%) (user's accuracy)				80.3	75.7	98.4
OVERALL CLASS PERFORMANCE (2179/2314)=94.2% Kappa Statistic(x100)=84.3% Kappa Variance=0.000144						

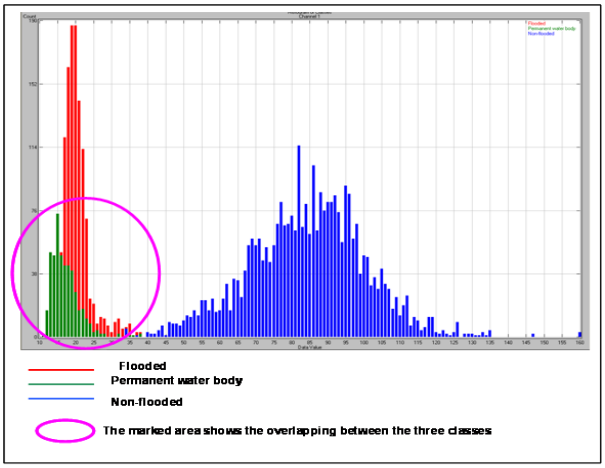

Figure 5. Histogram showing the overlapping in the class values

In Figure 5, the histogram also clearly shows the overlapping in the data values of the permanent water body and flooded areas.

After a comparison of the final classified image with the original image it can be seen that some river portion is classified as a flooded area and some flooded portions are also misclassified as river or permanent water bodies (Figure 6).

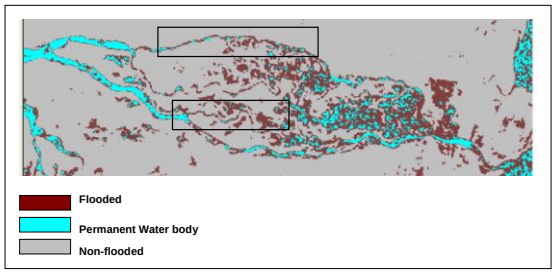

Figure 6. The classification of the image to extract the permanent water body from flooding

4.2. Unsupervised classification

Another attempt has been made to classify the radar image using clustering function. This classification process was run several times with changes in clustering parameters. Changing the number of clusters, the minimum cluster size and convergence (%) is helpful to distinguish the Permanent water body and Flooded area but to only a little extent. As in some classified images the flooded area is observed to be sub classed into several clusters and the same conditions occurred in case of river courses. In the case of non-flooded regions, several overlapped clusters were also observed. This might be due to the variation of moisture content in the soil, as mentioned before, since the whole study area is characterized by unpaved roads (Figure 9). Some of the results of the trial classifications are shown in Figure 7 and Figure 8, with the details of clustering parameters for all the attempts in Table 5.

Table 5. The listing of all the parameters used in the trial classification

Test	Parameters		
	Threshold	Convergence	Minimum Cluster Size
1	15	95	5
2	20	90	10
3	40	90	10

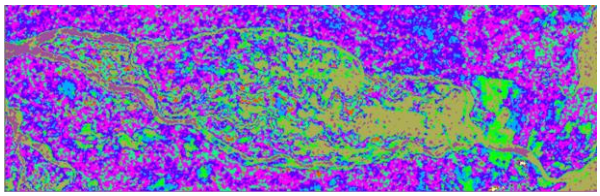

Figure 7. Test 1 using clustering function

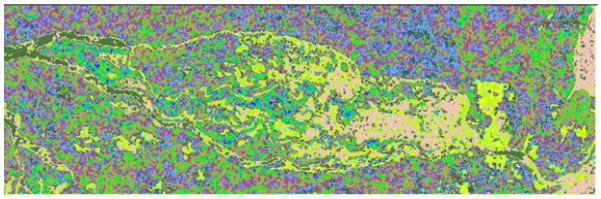

Figure 8. Test 2 using clustering function

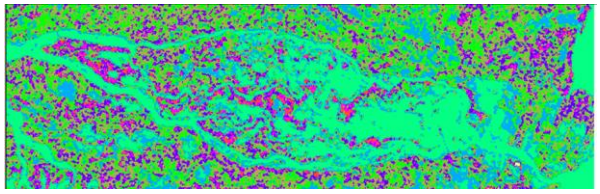

Figure 9. Test 3 using clustering function

4.3. Decision fusion with NDVI image

As discussed, while using conventional classification techniques it is easy to distinguish between the flooded and non-flooded portions; due to the similar reflectance it is difficult to extract the permanent water bodies from flooding. Even some water bodies were wrongly classified as non-flooded or land areas. These are mainly vegetation-covered small ponds (based on field observation) and thus giving brighter reflections like land areas.

To avoid this difficulty, a pre flood optical Landsat ETM image of the study area was used to extract the permanent water body. This attempt was taken with the aim of using the resultant image along with the

classified image of flooded and non-flooded areas to improve the accuracy of the flooding extent.

Bands 4, 3 and 2 of the ETM image were used. They firstly were co-registered with the Radar image using an affine function. Then using the NDVI algorithm, the NDVI image was extracted (Figure 10).

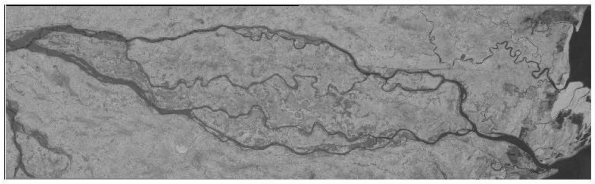

Figure 10. Normalized Difference Vegetation Index (NDVI) results

Pixel values were examined from this image and it was found that the value of NDVI ranges between -1 and +1. The vegetated area in this image appeared brighter as vegetation reflects near infrared and water in this image appeared darker toned. The value also varies within these two classes. The value for water with no vegetation was low and negative and non-water vegetated areas were highest. A threshold was chosen at -0.2 through studying the scatter plot of NIR and RED bands. Generally the non-water vegetation value should be positive in an NDVI image. Due to moisture content in the land the value dropped to below -0.2, but was still greater than the value of river. In the resultant image (Figure 11) only permanent water bodies were extracted.

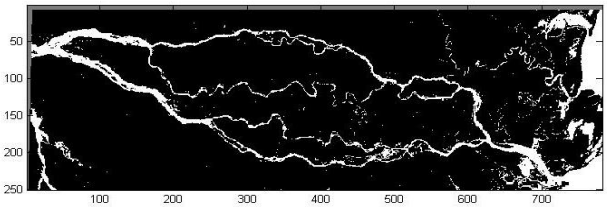

Figure 11. The Thresholded NDVI image

Finally the result from the optical image was fused with the classified image, derived from the radar data.

The concept of Theory of Evidence was applied in the decision fusion procedure. The essence of the technique involves the assignment of belief, represented as a mass of evidence, to various labeling propositions for a pixel. The total mass of evidence available for allocation over the candidate labels for the pixel is unity. If the quality of data or labeling process is slightly uncertain, the uncertainty about the labeling process can also be considered in this function [6].In this study the uncertainties are considered in extreme cases.

Since the optical data was acquired before the flood event, the labeling results have 0% uncertainty for permanent water and 100% for flooded or non flooded classes. For the radar data, it is reasonable to believe that the classified image has 100% uncertainty for the permanent water body extraction and flooded areas, but 0% uncertainty for the non flooded areas. As results, if the label given by the thresholded NDVI result is Permanent Water, the fusion result will be Permanent water. If the label given by the radar result is Non- flooded, the fusion result will be Non-flooded. If a pixel is not labeled as either, it will be classified as Flooded. The final mapping result is as shown Figure 12.

In Figure 12, it can be observed that flooding mainly occurred along the river banks and in the eastern portion of the river course which matches the ground truth information better than the individual classification on the optical and radar images. The accuracy of the final output image was tested against the accuracy of the classified Radar image. In both the cases of training data and testing data, this resultant fused image was proved to be able to improve the accuracy level. The training accuracy was increased from 88.7% to 91.14% and the testing accuracy was increased from 94.2% to 95.89%. Though several descriptive measures can be obtained from the Error Matrix, one of the most reliable measures for accuracy check is the Kappa Coefficient. Kappa ($\hat{k}$) statistic is actually a measure of agreement or accuracy. This measure of agreement is based on the difference between the actual agreement in the error matrix (i.e. the agreement between the remotely sensed classification and the reference data as indicated by the major diagonal) and the chance agreement which is indicated by the row and column totals [7]. The KAPPA statistic goes up from 77.8 % to 82.73% and 84.3% to 89.01% for training and testing data respectively. The increased accuracy of permanent water body class caused the increase in KHAT value for the final fused image.

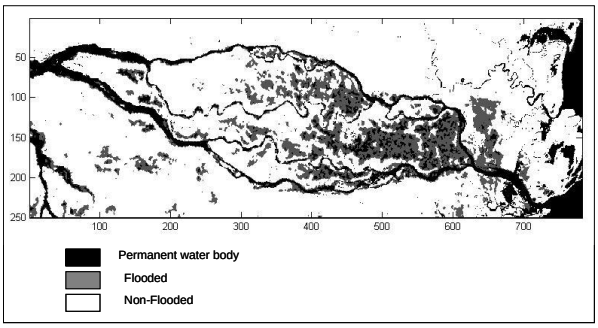

Figure 12. The final fused image

5. Conclusion

In this work, it was found to be difficult to differentiate the existing water body from the flooded areas. However, using the NDVI index, it was possible to extract most of the river body. The land area is muddy and always holds moisture to some extent because the study area falls under the monsoon regions of India. Occurrences of rainfall are thus very common phenomena, which cause complex reflectance of the land areas and lead to misclassification. When we tried to classify first the Radar image into water and non-water level, classification did not provide satisfactory results while trying to find the existing water masses. The problem is addressed by using the optical pre-flood image. The decision fusion results reduced the errors. Accuracy can be further increased by using the immediate pre-flood radar or multi-spectral imagery with good resolution.

6. Acknowledgement

This study was carried out considering the problems encountered during the dissertation in Masters conducted under the supervision of Dr. S.P. Aggarwal, V. Hariprashad, Mr. Praveen Thakur and Mr. Ashutosh Bhartwaj, with Indian Institute of Remote Sensing and Drs. Dinand Alkema, Drs. Nanette Kingma with International institute of Geoinformation Science and Earth Observation, The Netherlands. The authors would also like to thank the Indian Institution of Remote Sensing for providing the Radarsat satellite image.

7. References

[1] Middelmann, M.H., *Natural Hazards in Australia, Identifying Risk Analysis Requirements*, Geoscience Australia, 2007, pp: 60-79.

[2] Y. Wang, J.D. Colbey, and K.A. Mulcahy, "An Efficient Method for Mapping Flood Extent in a Coastal Floodplain using Landsat TM and DEM Data", *International Journal of Remote Sensing*, Taylor and Francis, London, 2002, pp. 3681-3696.

[3] Lillesand, T.M., and R.W. Keifer, *Remote Sensing and Image Interpretation*, John Wiley and Sons, Inc, United States of America, 2000.

[4] D.N. Davis, K. Natarajan, and E. Claridge, "Multiple energy function active contours applied to CT and MR images", *Image Processing and its Applications*, IEEE Xplore, Birmingham University, UK, 1995.

[5] M.S Horritt, and D.C. Mason, "Flood boundary Delineation from Synthetic Aperture Radar Imagery using a statistical active contour model", *International Journal of Remote Sensing*, Taylor and Francis, London, 2001, pp. 2489-2507.

[6] Richards, J.A., and X. Jia, *Remote Sensing Digital Image Analysis, an Introduction*, Springer, New York, 2006.

[7] Congalton R.G. and K.Green, *Assessing the Accuracy of Remotely Sensed Data: Principles and Practices*, Lewis, United States of America, 1999.